



Parcellation-based tractographic modeling of the ventral attention network

Parker G. Allan^a, Robert G. Briggs^b, Andrew K. Conner^a, Christen M. O'Neal^a, Phillip A. Bonney^b, B. David Maxwell^a, Cordell M. Baker^a, Joshua D. Burks^c, Goksel Sali^a, Chad A. Glenn^a, Michael E. Sughrue^{d,*}

^a Department of Neurosurgery, University of Oklahoma Health Science Center, Oklahoma City, OK, United States of America

^b Department of Neurosurgery, University of Southern California, Los Angeles, CA, United States of America

^c Department of Neurosurgery, Miami Miller School of Medicine, Miami, FL, United States of America

^d Center for Minimally Invasive Neurosurgery, Prince of Wales Private Hospital, Sydney, Australia

ARTICLE INFO

Keywords:
Anatomy
Attention
Parcellation
Tractography

ABSTRACT

Introduction: The ventral attention network (VAN) is an important mediator of stimulus-driven attention. Multiple cortical areas, such as the middle and inferior frontal gyri, anterior insula, inferior parietal lobule, and temporo-parietal junction have been linked in this processing. However, knowledge of network connectivity has been devoid of structural specificity.

Methods: Using relevant task-based fMRI studies, an activation likelihood estimation (ALE) of the VAN was generated. Regions of interest corresponding to the HCP cortical parcellation scheme were co-registered onto this ALE in MNI coordinate space and visually assessed for inclusion in the network. DSI-based fiber tractography was performed to determine the structural connections between cortical areas comprising the VAN.

Results: Fourteen regions within the right cerebral hemisphere were found to overlap the ALE of the VAN: 6a, 6r, 7AM, 7PM, 8C, AVI, FOP4, MIP, p9-46v, PCV, PFm, PGi, TPOJ1, and TPOJ2. Regions demonstrated consistent U-shaped interconnections between adjacent parcellations, and the SLF was found to connect frontal and parietal areas of the network.

Conclusions: We present a tractographic model of the VAN. This model comprises parcellations within the frontal and parietal cortices that are linked via the SLF. Future studies may refine this model with the ultimate goal of clinical application.

1. Introduction

Advances in human neuroimaging have revealed that the cerebral cortex is composed of complex, interacting neural networks [1–3]. This has led in part to the development of a two-network model of cortical attention [4,5]. One of these two attention networks, the ventral attention network (VAN), is involved in reorienting attention when a new, unexpected stimulus is detected within the environment [5,6].

Recent studies have characterized the cortical inputs of the VAN. The VAN is considered a right lateralized network that comprises parts of the inferior parietal lobule, temporo-parietal junction, anterior insula, inferior frontal gyrus, and middle frontal gyrus [7–10]. While important, existing descriptions of the VAN lack tractographic detail and offer limited insight into the underlying structural connections of the network. Task-based functional magnetic resonance imaging (fMRI)

and deterministic fiber tractography have made it possible to study the VAN in greater structural and functional detail [8,10–20]. In addition, newly published parcellated brain maps allow us to study network anatomy using a standard cortical atlas and nomenclature [21].

In this study, we constructed a model of the VAN based on the cortical parcellation scheme previously published under the Human Connectome Project (HCP) [21]. Using relevant task-based fMRI studies and BrainMap (<http://www.brainmap.org/>), a collection of open-access software programs used to generate activation likelihood estimations of neural networks, we identified the cortical areas involved in the VAN. After identifying the relevant cortical areas of interest, we performed DSI-based fiber tractography to determine the structural connections between regions of the network. Our goal is to provide a more detailed anatomic model of the VAN for use in future studies.

* Corresponding author at: Level 7 Prince of Wales Private Hospital, Suite 3, Barker Street, Randwick, New South Wales 2031, Australia.
E-mail address: sughruevs@gmail.com (M.E. Sughrue).

Table 1

Studies used to generate the activation likelihood estimation of the ventral attention network.

Study	Task	Number of participants	Study coordinate space	Coordinates used in the Meta-analysis (x, y, z)		
Chen et al. [25]	Invalidly cued reorienting of attention	20	MNI	52	-42	15
				-26	-68	25
				30	-74	31
				-18	-68	59
				18	-62	55
				36	-48	53
				30	-6	53
				4	-56	53
				-50	-66	3
				-45	3	-3
Coull et al. [26]	Invalidly cued reorienting of attention	6	Talairach	-30	30	-18
				33	21	-15
				-54	30	3
				45	24	6
				-57	-51	30
				20	10	54
				40	4	44
				42	12	30
Doricchi et al. [27]	Invalidly cued reorienting of attention	24	Talairach	60	-46	28
				12	-56	48
				34	-42	42
				29	-60	-14
				-31	-63	-15
				31	-81	4
				-29	-81	7
				25	-62	47
Downar et al. [28]	Passive observation of visual, auditory, and tactile stimuli	10	Talairach	53	-21	5
				-51	-37	10
				-53	-15	3
				50	-28	25
				-59	-28	27
				54	-42	13
				-54	-48	10
				57	-57	2
				43	6	5
				-51	-8	5
				-8	4	41
				27	18	10
				36	-16	6
				-39	15	33
				-63	-54	0
				57	-45	18
Gillebert et al. [29]	Invalidly cued reorienting of attention	16	MNI	39	0	39
				-48	-48	33
				3	63	51
				52	-62	6
				-46	-74	10
				56	18	26
				-49	19	18
				45	14	19
Han and Marois [12]	Searching for a target in a rapid serial visual presentation of distractors	14	Talairach	-55	-46	13
				49	-54	17
				-30	18	0
				28	16	0
				-2	15	44
				20	-66	54
				-14	-64	56
				-40	-40	40
Heinen et al. [13]	Spatial attention shifting task	16	MNI	-28	-6	48
				4	-56	54
				36	-40	40
				50	6	34
				-10	-48	52
				32	-6	60
				-28	-74	22
				-30	-50	46
				-46	4	26
				4	8	50
				34	-50	44
				52	-32	40
				-58	-34	34
				34	-76	22
				58	-36	26
				36	20	8

(continued on next page)

Table 1 (continued)

Study	Task	Number of participants	Study coordinate space	Coordinates used in the Meta-analysis (x, y, z)
Indovina et al. [30]	Invalidly cued reorienting of attention	3	MNI	-22 8 -6
				24 12 -2
				62 -36 34
				42 2 58
				54 8 22
				40 32 42
				52 18 -2
				6 -58 50
				-64 -40 32
				-36 -54 46
Indovina et al. [31]	Invalidly cued reorienting of attention	12	MNI	-30 -58 44
				34 -68 38
				-42 6 32
				48 14 26
				-8 -74 42
				8 -60 52
				-32 24 -8
				34 26 -4
				8 20 40
				-6 18 46
Johnston et al. [32]	Attentional Blink Task	16	Talairach	-30 4 54
				26 4 46
				50 1 43
				-42 -16 43
				30 -28 56
				26 25 55
				-21 -10 64
				-6 -13 56
				33 27 49
				49 0 46
Joseph et al. [8]	Invalidly cued reorienting of attention	20	MNI	-43 44 20
				60 4 18
				27 -64 21
				-36 -50 28
				33 -29 46
				29 -74 -2
				49 8 -7
				51 -54 21
				49 -39 5
				48 32 7
Kincade et al. [14]	Exogenous orienting of attention	20	Talairach	33 -73 19
				-28 -74 20
				9 -80 23
				43 -53 42
				36 -77 -19
				0 -22 66
				-35 -78 -31
				54 -40 6
				72 -30 2
				66 -42 30
Konrad et al. [33]	Attention Network Task Paradigm	16	Talairach	68 -36 0
				60 -52 32
				62 -42 -4
				14 -68 46
				33 -78 28
				51 -51 26
				48 12 12
				26 -6 60
				-57 -43 31
				54 -48 30
Lyu et al. [34]	Multiple Identity Tracking Task	19	MNI	-32 14 -1
				35 18 7
				-25 -13 45
				-25 -11 55
				27 -7 60
				9 2 56
				39 32 -7
				59 -40 13
				36 -43 66
				-21 -58 58

(continued on next page)

Table 1 (*continued*)

Study	Task	Number of participants	Study coordinate space	Coordinates used in the Meta-analysis (x, y, z)		
Macaluso et al. [35]	Invalidly cued reorienting of attention in multiple modalities	8	Talairach	6 -30 40 -39 54 -22 39 6 -47 -8 -33 36	-72 10 10 25 22 -69 -57 -63 -40 4 24 33	0 58 48 -1 -3 40 54 -2 9 30 -3 -9
Mastroberardino et al. [15]	Invalidly cued reorienting of attention	39	MNI	64 -58 34 -46 44 58 40	-40 -52 24 22 28 -46 -54	32 28 -18 0 22 20 40
Mattler et al. [36]	Perceptual and motor cuing tasks	12	MNI	4 8 4 20 0 52 48 60 56 4 -12 16 -56 -40 -44 44 40 40 4 -28 -8 36 -28 -8 36 24 -56 -52 -28 32 -84 -64 16 0 -44 12 0 20 36 -80 12 -64 -80 12 -64 56 -52 -28 -8 -1 16 -45 -45 -64 -80 -61 -64	28 16 36 8 -72 -56 -52 -52 -20 -76 -84 -64 16 0 8 12 0 40 20 40 36 -80 12 -64 -80 12 -64 24 -27 -41	40 60 49 69 36 32 40 4 -20 32 28 24 28 28 40 40 48 28 56 36 36 28 56 36 24 -24
Mayer et al. [38]	Invalidly cued reorienting of attention	17	Talairach	-52 32 -34 54 -59 16 -4 -28 21	3 -1 16 -45 -45 -68 -80 -61 -64	26 53 4 8 12 36 28 5 -27 -41
Mayer et al. [37]	Invalidly cued reorienting of attention	27	Talairach	1 17 -31 28 -32 41 -44 40 55 -55 16 -14 38 -38 57 10 -14 -11 -11 19	8 29 -6 -3 -19 11 3 13 -43 -45 -66 -67 -48 -44 -47 -3 -10 -70 -40 -56	50 -8 53 56 55 28 31 3 8 13 44 49 42 42 26 9 7 -30 -40 -33

(continued on next page)

Table 1 (continued)

Study	Task	Number of participants	Study coordinate space	Coordinates used in the Meta-analysis (x, y, z)		
Santangelo et al. [16]	Invalidly cued reorienting of attention	17	MNI	-29 8 48 58 52 46 14 14 36 45 10 6 10 6 52 22 17 35 45 44 37 25 5 4 3 19 4 10 6 4 45 39 39 29 11	-56 16 22 -52 -48 -45 -57 -60 -62 -48 -65 -38 -62 -46 -39 10 47 11 27 12 28 33 35 20 46 55 23 37 45 0 3 56 35 49 24 33 42 45 50 57 41 16 45 20 32 37 35 25 -7 3 -7 10	-37 64 34 36 14 26 23 14 45 37 55 34 37 0 3 56 35 49 24 33 42 45 50 57 41 16 45 20 20 1 29 9 -7 3 -7 6
Shulman et al. [10]	Invalidly cued reorienting of attention	24	Talairach			
Veldhuizen et al. [17]	Receipt of expected and unexpected-tasting solutions	22	MNI	-36 -33 -33 33 48 48 42 -6 6 9 15 -6 -12 3 42 12 42 -27 48 -6 57 66 -6 3 6 9 -45 -6 -48 48 48 39 -33 51 -45 0 -9 -27 6	18 12 30 21 21 30 0 24 36 36 42 -9 3 -12 3 6 30 45 -51 36 -30 -33 -24 -15 -24 -66 42 6 18 30 21 18 -69 -48 15 3 21 -9 45 27	0 -6 6 -3 24 24 30 39 51 9 3 39 6 3 45 6 39 -9 0 -6 3 45 3 21 30 30 18 9 42 21 30 18 -6 30 24 30 18 9 21 36 -6 15 30 15 18

(continued on next page)

Table 1 (continued)

Study	Task	Number of participants	Study coordinate space	Coordinates used in the Meta-analysis (x, y, z)
Vossel et al. [39]	Invalidly cued reorienting of attention	16	MNI	6 45 39 33 21 -6 33 9 -9 -33 18 0 -33 9 -6 33 27 3 36 18 6 -42 -9 -6 -27 45 15 6 27 18 48 -27 -9 54 -33 -6 0 -39 -9 0 -12 3 -15 -12 9 0 -21 3 -33 48 -9 -21 57 -3 12 9 9 18 0 6 12 3 15 9 -66 39 9 -78 36 -9 -27 -12 63 -33 -18 -36 30 6 -27 12 -18 24 48 -9 -51 -45 48 15 -72 21 -51 36 15 48 36 -12 -9 -75 -33 -24 -63 39 12 -33 9 6 -21 36 -12 3 6 54 -48 45 57 -57 15 45 -45 21 51 -39 30 45 -45 18 57 -57 15 66 -40 9 -58 -54 13 44 -62 13 20 -72 59 50 36 17 36 20 -7 -42 -36 53 -50 -62 -15 50 -58 -17 -30 -36 -27 54 12 41 32 -66 51 -7 -52 50 -7 -69 58 -10 24 -14 -38 17 -4 45 10 0 -14 41 27 10 28 18 48 -65 14 55 -55 4 -38 -26 46 48 -74 0 12 10 38 -16 -56 -44 -2 -24 -44 -32 40 20 -32 -52 -30 0 -6 52 -40 -66 -6 -58 4 32 56 -58 10
Vossel et al. [40]	Invalidly cued reorienting of attention	24	MNI	66 -40 9 -58 -54 13 44 -62 13 20 -72 59 50 36 17 36 20 -7 -42 -36 53 -50 -62 -15 50 -58 -17 -30 -36 -27 54 12 41 32 -66 51 -7 -52 50 -7 -69 58 -10 24 -14 -38 17 -4 45 10 0 -14 41 27 10 28 18 48 -65 14 55 -55 4 -38 -26 46 48 -74 0 12 10 38 -16 -56 -44 -2 -24 -44 -32 40 20 -32 -52 -30
Weissman and Prado [18]	Invalidly cued reorienting of attention	17	MNI	-7 -52 50 -7 -69 58 -10 24 -14 -38 17 -4 45 10 0 -14 41 27 10 28 18 48 -65 14 55 -55 4 -38 -26 46 48 -74 0 12 10 38 -16 -56 -44 -2 -24 -44 -32 40 20 -32 -52 -30
Wynn et al. [19]	Visual Oddball Task	22	MNI	-38 -26 46 48 -74 0 12 10 38 -16 -56 -44 -2 -24 -44 -32 40 20 -32 -52 -30
Xuan et al. [20]	Modified Attention Network Task Paradigm	24	MNI	0 -6 52 -40 -66 -6 -58 4 32 56 -58 10

(continued on next page)

Table 1 (continued)

Study	Task	Number of participants	Study coordinate space	Coordinates used in the Meta-analysis (x, y, z)
			34	-52 -16
			-22	-70 28
			-26	-8 62
			54	6 34
			-26	-50 54
			30	-8 54
			26	-74 26
			24	-58 52
			-8	12 38
			-38	-38 36
			34	-82 2
			-56	-22 48
			46	-26 46
			-24	-50 -28
			-6	-68 -22
			12	-10 6
			-14	-18 8
			34	12 0
			20	-54 6
			-26	-92 0
			-14	-56 4
			6	-82 2
			10	-20 -44
			-18	10 -10
			56	-38 26
			56	-14 20
			8	-58 -42
			22	12 2
			26	-34 -40
			24	36 24
			-2	-38 54
			-30	14 8
			2	-34 -20
			-40	28 10
			-44	24 34
			30	2 -8
			38	-52 54
			8	-54 54
			-40	-48 58
			58	-44 40
			-48	-42 30
			38	-72 32
			-20	-66 52
			34	0 48
			38	26 36
			44	36 12
			52	12 14
			18	16 58
			-16	-42 -46
			-36	-70 -26
			38	46 -8
			28	-70 -24
			36	-48 -26

2. Methods

2.1. Literature search

We initially searched for relevant task-based fMRI studies related to the VAN in BrainMap Sleuth 2.4 [22–24]. No research articles were identified using this software. We subsequently queried PubMed on July 12, 2017 for fMRI studies relevant to the VAN. We used the following search algorithm: “ventral attention network OR VAN OR stimulus driven attention network AND fMRI”. Studies were included in our analysis if they fulfilled the following search criteria: (1) peer-reviewed publication, (2) task-based fMRI study related to the ventral attention network or stimulus-driven attentional processing, (3) based on whole-brain, voxel-wise imaging, (4) including standardized coordinate-based results in the Talairach or Montreal Neuroimaging Institute (MNI) coordinate space, and (5) including at least one healthy

human control cohort. Studies related to the dorsal attention network were excluded. Only coordinates from healthy subjects were utilized in our analysis. Overall, 28 papers met criteria for inclusion in this study [8,10–20,25–40]. The properties of these studies are summarized in Table 1.

2.2. Creation of 3D regions of interest

In the original HCP study, parcellation data were studied in CIFTI file format. CIFTI files involve a surface-based coordinate system, termed greyordinates, which localizes regions of interest (ROIs) on inflated brains [41]. This is in contrast to traditional file formats, such as NIFTI, which denote regions based on volumetric dimensions [42]. As a result, it was difficult to perform deterministic fiber tractography using ROIs in CIFTI file format. To convert parcellation files to volumetric coordinates, the relevant greyordinate parcellation fields were

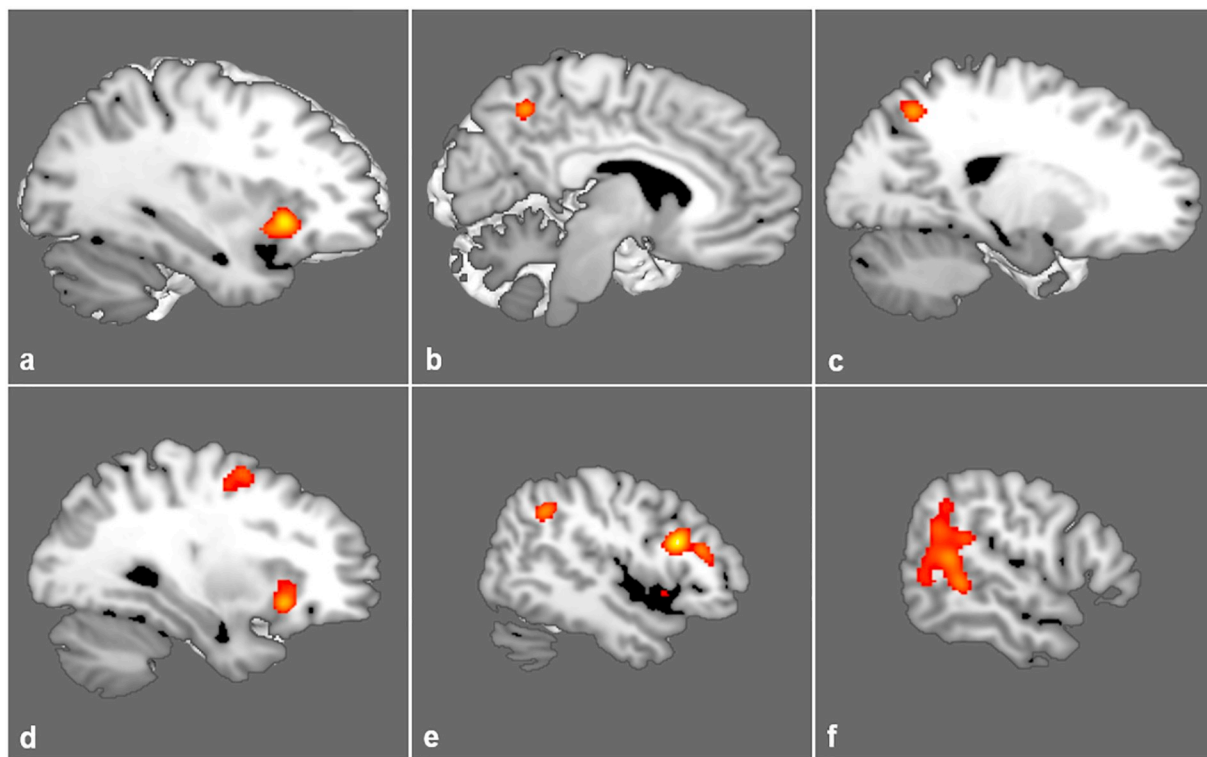


Fig. 1. Activation likelihood estimation (ALE) of 28 task-based fMRI experiments related to stimulus-driven attentional processing. The three-dimensional ALE data are displayed in Mango on a brain normalized to the MNI coordinate space. (A) ALE data highlighting the anterior apex of the insula and frontal operculum. (B-C) ALE data highlighting the superior parietal cortex. (D-E) ALE data highlighting the inferior frontal gyrus and middle frontal gyrus. (F) ALE data highlighting the inferior parietal lobule and temporo-parietal junction.

standardized to the three-dimensional volumetric working spaces of DSI Studio (Carnegie Mellon, <http://dsi-studio.labsolver.org>) using structural imaging data available through the HCP. This operation was performed using the Connectome Workbench command line interface (Van Essen Laboratory, Washington University 2016). A single, volumetric ROI was generated for the parcellations identified in the original HCP study [21].

2.3. ALE generation and identification of relevant cortical regions

We used BrainMap GingerALE 2.3.6 to extract the relevant fMRI data from the aforementioned studies to create an activation likelihood estimation (ALE) [43–45]. All Talairach coordinates identified during literature review were converted to the MNI coordinate space using SPM Conversion in GingerALE. We subsequently performed a single study analysis using cluster-level inference in the MNI coordinate space (cluster level of 0.05, threshold permutations of 1000, uncorrected *p*-value of 0.001). The ALE coordinate data were displayed on an MNI-normalized template brain using the Multi-image Analysis GUI (Mango) 4.0.1 (ric.uthscsa.edu/mango). The pre-constructed ROIs of the parcellations were then overlaid on the ALE and compared visually for inclusion in the network.

2.4. Network tractography

Publicly available imaging data from the Human Connectome Project was obtained for this study (<http://humanconnectome.org>, release Q3). A random sample of 25 healthy, unrelated subjects was selected (Subjects IDs: 100307, 103414, 105115, 110411, 111312, 113619, 115320, 117112, 118730, 118932, 100408, 115320, 116524, 118730, 123925, 148335, 148840, 151526, 160123, 178950, 188347, 192540, 212318, 366446, 756055). Diffusion imaging from these subjects was analyzed to identify fiber tracks connecting parcellations

within the network. A multi-shell diffusion scheme was used, and the b-values were 990, 1985, and 1980 s/mm². Each b-value was sampled in 90 directions. The in-plane resolution was 1.25 mm. The diffusion data was reconstructed using generalized q-sampling imaging with a diffusion sampling length ratio of 1.25 [46].

All brains were registered to the Montreal Neurologic Institute (MNI) coordinate space [47], wherein imaging is warped to fit a standardized brain model comparison between subjects [47]. Tractography was performed in DSI Studio (Carnegie Mellon, <http://dsi-studio.labsolver.org>) using a region of interest approach to initiate fiber tracking from a user-defined seed region [48]. A two-ROI-approach was used to isolate tracts [49].

Voxels within each ROI were automatically traced with a maximum angular threshold of 45 degrees. When a voxel was approached with no tract direction or a direction change of greater than 45 degrees, the tract was halted. Tractography was terminated after reaching a maximum length of 800 mm. In some instances, exclusion ROIs were placed to exclude obvious spurious tracts that were not involved in the white matter pathway of interest.

2.5. Measuring tract strength and frequency

To quantify the strength of the connections identified within the VAN across all subjects, the tracking parameters used within DSI Studio were modified such that the program would count the total number of tracts between any two ROIs based on a random seed count of 2.5 million. Working sequentially through ROI pairs in the network, the number of tracts between regions was recorded for each of the 25 subjects after fiber tractography was terminated under these conditions. The strengths of the connections within the VAN were calculated by averaging the number of tracts between each ROI pair of the network across all subjects.

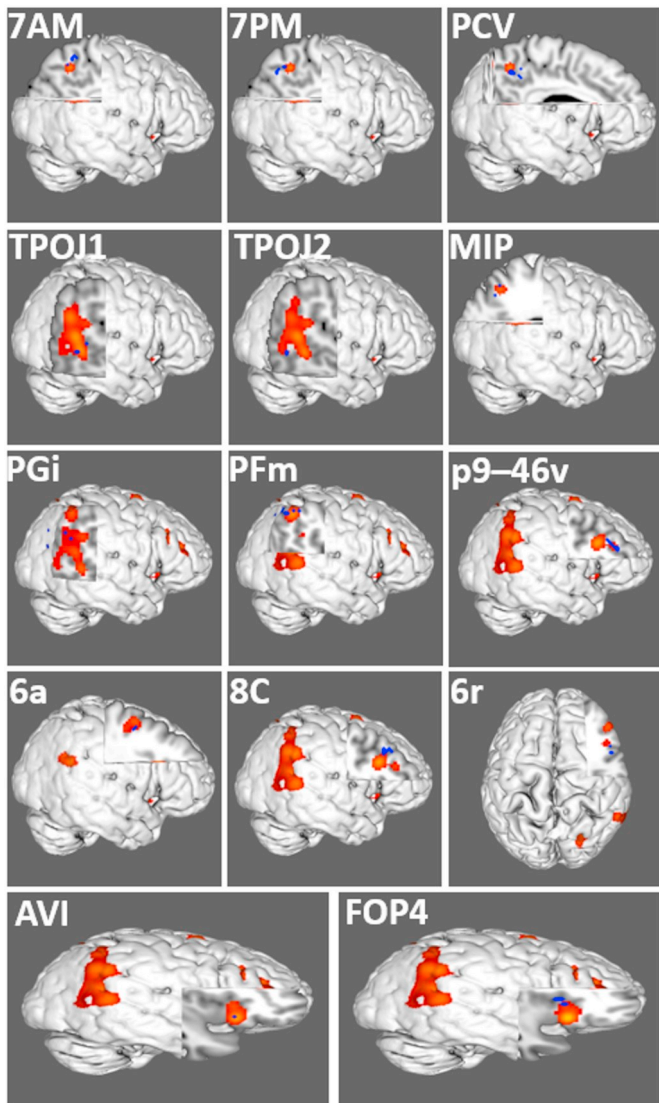


Fig. 2. Comparison overlays between the cortical parcellation data (blue) and activation likelihood estimation (ALE) data (red) from Fig. 1 in the right cerebral hemisphere. Cortical regions of interest were included in the network if they overlapped with the ALE data. Parcels included in the model of the ventral attention network were identified in the inferior frontal gyrus (6r and FOP4), anterior insula (AVI), middle frontal gyrus (6a, 8C, p9-46v), superior parietal lobule (7AM, 7PM, and MIP), inferior parietal lobule (PFm, PGi), and temporo-parietal junction (TPOJ1, and TPOJ2). The labels indicate the parcellation of interest within each panel. (For interpretation of the references to colour in this figure legend, the reader is referred to the web version of this article.)

3. Results

3.1. ALE regions and corresponding parcellations

Fig. 1 demonstrates the ALE of the 28 task-based fMRI experiments included in our meta-analysis of the VAN. Highlighted areas include the inferior frontal gyrus, middle frontal gyrus, anterior insula, superior and inferior parietal lobules, and temporo-parietal junction within the right cerebral hemisphere. Fourteen regions of interest were found to overlap the fMRI data, including 6a, 6r, 7AM, 7PM, 8C, AVI, FOP4, MIP, p9-46v, PCV, PFm, PGi, TPOJ1, and TPOJ2. Comparison overlays between the cortical parcellations and the ALE are shown in Fig. 2.

3.2. Structural connections within the ventral attention network

Deterministic tractography was utilized to show the basic structural connectivity of the VAN. An example of these results is shown in Fig. 3. Individual connections within the network are presented in Table 2 which tabulates the average strength of individual connections and lists the type-specific white matter connections identified between regions.

The cortical areas comprising the VAN can be classified based on the gyrus of the brain to which they localize, including the inferior frontal gyrus (6r, FOP4), the anterior insula (AVI), the middle frontal gyrus (6a, 8C, p9-46v), the superior parietal lobule (7AM, 7PM, PCV, MIP), the inferior parietal lobule (PFm, PGi), and temporo-parietal junction (TPOJ1, TPOJ2). U-shaped fibers form a majority of the connections between ROI pairs within the network. These fibers each have a similar morphology. They originate from one part of the cortex, curve 180 degrees across a sulcus, and terminate in a part of the brain immediately adjacent to their origin. These fibers represent the local connections between frontal and parietal components of the network.

The superior longitudinal fasciculus (SLF) connects multiple areas within the VAN. The SLF projects between frontal and parietal areas of the network as it courses within the deep white matter underneath the sensorimotor cortex around the Sylvian fissure. The principle projections of the SLF arising from frontal regions within the VAN include areas 6a, 6r, 8C FOP4, and p9-46v. Each tract has essentially the same morphology, with fibers coursing into the deep white matter of the posterior frontal lobe. These fibers then pass deep to the motor and sensory strips before bending 90 degrees supero-laterally to terminate within parcellations of the parietal lobe and temporo-parietal junction.

The connections of the VAN are summarized in Fig. 4. Lines in this schematic represent individual connections within the network. They are labeled with their average strength as measured across all 25 subjects included in this analysis.

4. Discussion

In this study, we utilized meta-analytic fMRI software and deterministic fiber tractography in order to construct a structural model of the VAN. This model is based on the cortical parcellation scheme previously published under the Human Connectome Project [21]. The VAN is known to mediate attentional processes within the right cerebral hemisphere [4–7,50], including reorientation of attention in the presence of unexpected, behaviorally-relevant stimuli [4–6]. The anatomic constituents of this network are discussed below.

4.1. Cortical regions of the middle frontal Gyrus

The middle frontal gyrus in the right cerebral hemisphere forms part of the VAN [7,50]. This gyrus is thought to mediate aspects of the dynamic interactions that occur between the ventral and dorsal attention networks within the brain [7], suggesting the middle frontal gyrus represents an important hub region for attentional processing. While evaluating cortical regions for inclusion in the VAN, we found that parcellations 6a, 8C and p9-46v overlap the ALE in the region of the right middle frontal gyrus.

Area 6a occupies the superior frontal sulcus, extending superiorly and inferiorly onto the middle and superior frontal gyri. Little is known about its function, although it likely participates in premotor planning [51]. In contrast to area 6a, area 8C localizes to the middle frontal gyrus proper, with the inferior frontal sulcus forming part of its inferior boundary. Area p9-46v borders 8C anteriorly. Functionally, area 8C is involved in the interpretation and maintenance of complex visuospatial information [52,53], while area p9-46v is involved in the higher-order cognitive processes linked to volitional behavior [54,55].

These three regions likely play additional roles in stimulus-driven attentional processing given their overlap with the VAN. However, their relevance to the network remains poorly understood. Some have

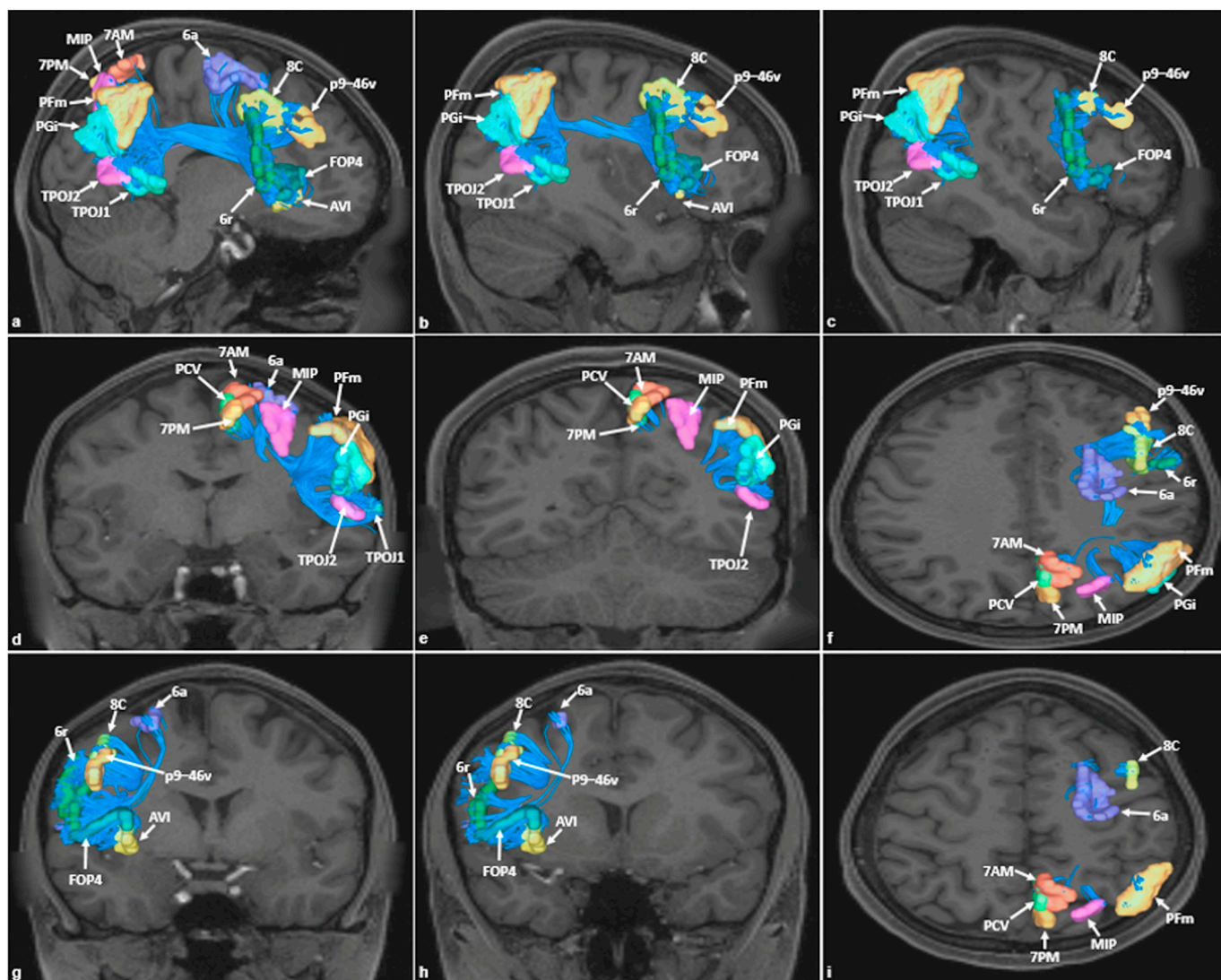


Fig. 3. Fiber tracking analysis for the ventral attention network. Shown on T1-weighted MR images in the right cerebral hemisphere. (A-C) Sagittal sections from most medial to most lateral demonstrating the superior longitudinal fasciculus and its projections between the frontal and parietal regions of the ventral attention network. (D-E) Coronal sections through temporal and parietal regions demonstrate local U-shaped fibers connecting adjacent areas within the posterior aspect of the network. (F-G) Coronal sections through the frontal regions demonstrate local U-shaped fibers connecting adjacent areas within the anterior aspect of the network. (H-I) Axial sections through the network re-demonstrate the superior longitudinal fasciculus as it courses between frontal and parietal areas.

proposed that the VAN acts as a circuit-breaker to disrupt voluntary attentional processing when unexpected stimuli are detected in the environment [5]. Whether these regions co-activate within the VAN to reorient spatial attention to the stimulus or re-direct motor behavior to respond to the stimulus is unclear. In addition, some studies have demonstrated that components of the VAN activate when stimuli are detected at an expected location [56,57]. Thus, while attention shifts to the stimulus, spatial orientation may not change, a process that may be mediated in part by frontal lobe parcellations within the VAN.

All three middle frontal gyrus areas are interconnected via U-shaped fiber bundles. These regions also demonstrate projections via the SLF to parcellations in the inferior parietal lobule and temporo-parietal junction, two parts of the cortex identified as part of the VAN [8,9,58–61]. Identification of the SLF within our model of the VAN is consistent with reports describing the anatomy of attention-related neurologic deficits, such as neglect, which is thought to occur from disruption to the underlying white matter pathways interconnecting the frontal and parietal cortices in the right cerebral hemisphere [62–65].

4.2. Cortical regions of the inferior frontal gyrus and opercular-insular cortex

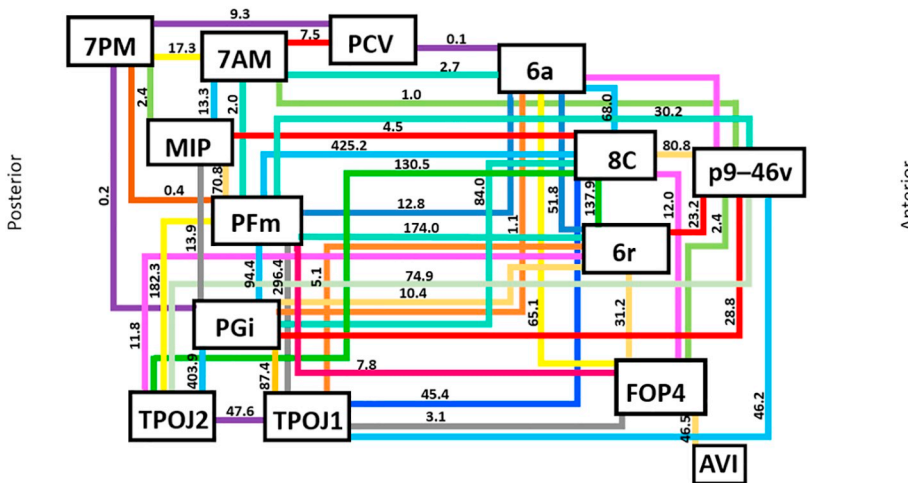
The inferior frontal gyrus and opercular-insular cortex also comprise the VAN [9,14,17,66]. Candidate parcellations found to overlap the ALE within these parts of the brain include 6r, FOP4, and AVI. Area 6r is located on the posterior-most aspect of the pars opercularis on the lateral surface of the inferior frontal gyrus. FOP4 is located on its inner surface within the frontal operculum. Area AVI forms the inferior border of the frontal operculum, and localizes to the anterior apex of the insula. Based on our model of the VAN, these regions are locally connected via U-shaped fibers to each other and the parcellations of the middle frontal gyrus. Area FOP4 has structural connections to parietal lobe regions via the SLF.

Few studies have examined the specific functional roles of these areas. This is largely related to their recent delineation under the HCP [21]. However, it is known that several of these regions (6r, FOP4) are variably involved in language initiation and production within the left cerebral hemisphere [67–70]. Similarly, the anterior insula is involved in multiple cortical functions not necessarily related to attention,

Table 2

Type and strength of connections within the ventral attention network.

Connection	Number of subjects	Average strength weighted by all subjects	Average strength weighted by identified subjects	Connection type
6a to 6r	22/25 (88%)	51.8	58.8	U-shaped fiber
6a to 7 AM	5/25 (20%)	2.7	13.6	SLF
6a to 8C	18/25 (72%)	68.0	94.4	U-shaped fiber
6a to FOP4	13/25 (52%)	65.1	125.2	U-shaped fiber
6a to p9-46v	6/25 (24%)	3.0	12.5	U-shaped fiber
6a to PCV	1/25 (4%)	0.1	2.0	SLF
6a to PFm	13/25 (52%)	12.8	24.6	SLF
6a to PGi	7/25 (28%)	1.1	4.0	SLF
6r to 8C	21/25 (84%)	137.9	164.1	U-shaped fiber
6r to FOP4	16/25 (64%)	31.2	48.7	U-shaped fiber
6r to p9-46v	13/25 (52%)	23.2	44.5	U-shaped fiber
6r to PFm	22/25 (88%)	174.0	197.8	SLF
6r to PGi	11/25 (44%)	10.4	23.7	SLF
6r to TPOJ1	5/25 (20%)	5.1	25.6	SLF
6r to TPOJ2	9/25 (36%)	11.8	32.9	SLF
7AM to 7 PM	12/25 (48)	17.3	36.0	U-shaped fiber
7AM to MIP	11/25 (44%)	13.3	30.3	U-shaped fiber
7AM to p9-46v	2/25 (8%)	1.0	12.0	SLF
7AM to PCV	16/25 (64%)	7.5	11.7	U-shaped fiber
7AM to PFm	7/25 (28%)	2.0	7.3	U-shaped fiber
7PM to MIP	6/25 (24%)	2.4	10.2	U-shaped fiber
7PM to PCV	16/25 (64%)	9.3	14.6	U-shaped fiber
7PM to PFm	2/25 (8%)	0.4	4.5	U-shaped fiber
7PM to PGi	2/25 (8%)	0.2	2.5	U-shaped fiber
8C to FOP4	6/25 (24%)	12.0	50.0	U-shaped fiber
8C to MIP	7/25 (28%)	4.6	16.6	SLF
8C to p9-46v	25/25 (100%)	80.8	80.8	U-shaped fiber
8C to PFm	22/25 (88%)	425.2	483.2	SLF
8C to PGi	20/25 (80%)	84.0	105.0	SLF
8C to TPOJ1	15/25 (60%)	45.4	75.6	SLF
8C to TPOJ2	21/25 (84%)	130.5	155.3	SLF
AVI to FOP4	24/25 (96%)	46.5	48.5	U-shaped fiber
FOP4 to p9-46v	4/25 (16%)	2.4	14.8	U-shaped fiber
FOP4 to PFm	11/25 (44%)	7.8	17.8	SLF
FOP4 to TPOJ1	8/25 (32%)	3.1	9.8	SLF
MIP to PFm	19/25 (76%)	70.8	93.2	U-shaped fiber
MIP to PGi	10/25 (40%)	13.9	34.8	U-shaped fiber
p9-46v to PFm	11/25 (44%)	30.2	68.7	SLF
p9-46v to PGi	10/25 (40%)	28.8	71.9	SLF
p9-46v to TPOJ1	10/25 (40%)	46.2	115.4	SLF
p9-46v to TPOJ2	11/25 (44%)	74.9	170.3	SLF
PFm to PGi	22/25 (88%)	94.4	107.2	U-shaped fiber
PFm to TPOJ1	23/25 (92%)	296.4	322.2	U-shaped fiber
PFm to TPOJ2	23/25 (92%)	182.3	198.1	U-shaped fiber
PGi to TPOJ1	17/25 (68%)	87.4	128.5	U-shaped fiber
PGi to TPOJ2	25/25 (100%)	403.9	403.9	U-shaped fiber
TPOJ1 to TPOJ2	22/25 (88%)	47.6	54.1	U-shaped fiber

**Fig. 4.** Simplified schematic of the white matter connections identified between individual parcellations of the ventral attention network during the fiber tracking analysis. Connections are labeled with the average strength measured across all 25 subjects used in the study.

including processes related to self-awareness and self-recognition [71,72]. While the precise role of these regions in attentional processing is not well understood, the right inferior frontal gyrus, frontal operculum, and insula have been shown to co-activate across multiple attention-related task-based fMRI studies [9,14,17,66], suggesting these regions are involved in stimulus-driven attention within the right cerebral hemisphere. Area AVI may also be involved in the cortical processing that occurs to increase recognition and awareness of a new stimulus in the environment.

4.3. Cortical regions of the inferior parietal lobule and temporo-parietal junction

The inferior parietal lobule and temporo-parietal junction also form part of the VAN [8,9,58–61]. Like the middle frontal gyrus, these areas are highlighted only within the right cerebral hemisphere in our ALE. This lateralization is consistent across other studies [8–10,59,60]. Candidate parcellations found to overlap the ALE within the inferior parietal lobule include regions PFm and PGi. Parcellations found to overlap the ALE within and temporo-parietal junction include TPOJ1 and TPOJ2. All of these areas localize to some part of the inferior parietal lobule. Area PFm is located in the angular gyrus and extends onto the posterior-most aspect of the supramarginal gyrus. Area PGi is located entirely within the angular gyrus. TPOJ1 is located within the superior temporal sulcus at the level of the angular gyrus, and borders TPOJ2 anteriorly. TPOJ2 forms part of the lateral occipital cortex, extending onto the posterior-inferior bank of the angular gyrus.

The regions comprising the inferior parietal lobule are associated with higher-order functional processes. Area PFm has been shown to be active in non-spatial, attention-related tasks, in particular those associated with reorientation and rule change during visually-guided tasks [73,74]. Similarly, PGi has been shown to be active during changes in visuospatial attention [75]. This region also forms part of the default mode network, which plays a role in re-directing attention towards internal stimuli [21]. While little is known regarding the function of individual parcellations within the temporo-parietal junction, this region is associated with salient and self-related processing within the cortex [76], and has been shown to play a role in detecting incongruities between different stimuli [76]. Taken together, the complex functional processes attributed to the inferior parietal lobule and temporo-parietal junction, including visuospatial processing, likely assist in reorienting attention to important stimuli detected in the environment. The VAN may also mediate some aspects of internal reorientation during resting state activity.

4.4. Cortical regions of the superior parietal lobule

The superior parietal lobule is not traditionally thought of as a node within the VAN. Instead, the superior parietal lobule is thought to mediate several important cortical processes related to sensorimotor integration [77–79], spatial perception [79,80], and visuospatial attention [5,81–84]. Despite this seeming incongruity, we have included parcellations of the superior parietal lobule within our model of the VAN which were found to overlap the network ALE, including areas 7AM, 7PM, MIP, and PCV.

Of these four regions, areas 7AM and 7PM have some role in visuospatial attention processing [79,85]. These regions are particularly involved in processing information related to space, shape and motion [79,85]. Area MIP, which is partially located within the intraparietal sulcus, is involved in the transformation of visual information into motor action plans [86,87], and area PCV, which is located in the superior aspect of the precuneus, is involved in visuospatial perception [88,89]. While these areas are clearly important in visuospatial processing and transforming this information into motor planning, their role within the VAN is not understood. It is possible that these regions form part of the dorsal attention network, given the role of the superior

parietal lobule and intraparietal sulcus in this network [5,81–84]. It may also be the case that the subcortical white matter pathways interconnecting the superior and inferior parietal lobules serve to transmit information between nodes of the dorsal and ventral attention networks. In our previous work modeling the dorsal attention network, we found that both 7AM and 7PC form part the parietal node within the dorsal attention network [90].

4.5. The strength of connections within the ventral attention network

The strength of the connections identified between parcellations of the VAN are reported in Table 2. Two different values for strength are recorded based on the average number of tracts across all subjects versus the average number of tracts across subjects in which the connection was identified. Based on these results, it is clear that the structural connectivity of the VAN varies to some degree between individuals. Thus, by presenting both sets of average connectional strengths, one can see how connections can vary in the network.

It should also be noted that we did not set a threshold for average strength when considering connections within the VAN. Setting such a threshold or a threshold related to tract frequency (i.e. how many times a tract is identified in subjects) would limit the type and variety of connections discussed in our model. In our view, this would be incorrect. Instead, it more appropriate to say that a certain connection is relatively weak or occurs infrequently in the network. Despite not setting a threshold, the frequency and strength associated with certain connections raise important questions regarding the significance of certain connections to the functionality of the network. Unfortunately, answering these questions is beyond the scope of this study. Future studies will need to examine the critical connections within the VAN most important for the functioning of the network.

4.6. Sensory modalities and the ventral attention network

Finally, attention-related experiments involving visual, auditory, and gustatory modalities were included in this analysis. Some neuroscientists have found evidence for a modality-specific VAN [91]. We recognize that different types of stimuli may recruit different areas of the brain when reorienting attention. However, in this study our aim was to identify the major cortical inputs of the VAN using an established cortical parcellation scheme. Furthermore, some studies suggests that areas such as the temporo-parietal junction and insula are active in attentional processing across multiple sensory modalities [17,59,92]. Future studies may explore the differences in VAN network topology across different attention-related tasks associated with different sensory modalities, and it is certainly possible that the model of the VAN proposed here may change based on these results.

5. Conclusions

We present a tractographic model of the ventral attention network. This model comprises parcellations within the frontal and parietal cortices within the right cerebral hemisphere that are principally linked through the superior longitudinal fasciculus. Future studies may refine this model with the ultimate goal of clinical application.

Disclosures

The authors report no conflict of interest concerning the materials or methods used in this study or the findings specified in this paper.

Funding

This research did not receive any specific grant from funding agencies in the public, commercial, or not-for-profit sectors.

Declaration of Competing Interest

None.

Acknowledgements

None.

References

- [1] M. De Luca, C.F. Beckmann, N. De Stefano, P.M. Matthews, S.M. Smith, fMRI resting state networks define distinct modes of long-distance interactions in the human brain, *NeuroImage* 29 (4) (2006) 1359–1367.
- [2] B. Thirion, S. Dodel, J.B. Poline, Detection of signal synchronizations in resting-state fMRI datasets, *NeuroImage* 29 (1) (2006) 321–327.
- [3] C.F. Beckmann, M. DeLuca, J.T. Devlin, S.M. Smith, Investigations into resting-state connectivity using independent component analysis, *Philos. Trans. R. Soc. Lond. Ser. B Biol. Sci.* 360 (1457) (2005) 1001–1013.
- [4] A.B. Chica, P. Bartolomeo, J. Lupianez, Two cognitive and neural systems for endogenous and exogenous spatial attention, *Behav. Brain Res.* 237 (2013) 107–123.
- [5] M. Corbetta, G.L. Shulman, Control of goal-directed and stimulus-driven attention in the brain, *Nat. Rev. Neurosci.* 3 (3) (2002) 201–215.
- [6] B. Hahn, T.J. Ross, E.A. Stein, Neuroanatomical dissociation between bottom-up and top-down processes of visuospatial selective attention, *NeuroImage* 32 (2) (2006) 842–853.
- [7] M. Corbetta, G. Patel, G.L. Shulman, The reorienting system of the human brain: from environment to theory of mind, *Neuron* 58 (3) (2008) 306–324.
- [8] R.M. Joseph, Z. Fricker, B. Keehn, Activation of frontoparietal attention networks by non-predictive gaze and arrow cues, *Soc. Cogn. Affect. Neurosci.* 10 (2) (2015) 294–301.
- [9] S. Vossel, R. Weidner, J. Driver, K.J. Friston, G.R. Fink, Deconstructing the architecture of dorsal and ventral attention systems with dynamic causal modeling, *J. Neurosci.* 32 (31) (2012) 10637–10648.
- [10] G.L. Shulman, D.L. Pope, S.V. Astafiev, M.P. McAvoy, A.Z. Snyder, M. Corbetta, Right hemisphere dominance during spatial selective attention and target detection occurs outside the dorsal frontoparietal network, *J. Neurosci.* 30 (10) (2010) 3640–3651.
- [11] C.M. Greene, D. Soto, Functional connectivity between ventral and dorsal frontoparietal networks underlies stimulus-driven and working memory-driven sources of visual distraction, *NeuroImage* 84 (2014) 290–298.
- [12] S.W. Han, R. Marois, Functional fractionation of the stimulus-driven attention network, *J. Neurosci.* 34 (20) (2014) 6958–6969.
- [13] K. Heinen, E. Feredoes, C.C. Ruff, J. Driver, Functional connectivity between pre-frontal and parietal cortex drives visuo-spatial attention shifts, *Neuropsychologia* 99 (2017) 81–91.
- [14] J.M. Kinrade, R.A. Abrams, S.V. Astafiev, G.L. Shulman, M. Corbetta, An event-related functional magnetic resonance imaging study of voluntary and stimulus-driven orienting of attention, *J. Neurosci.* 25 (18) (2005) 4593–4604.
- [15] S. Mastroberardino, V. Santangelo, E. Macaluso, Crossmodal semantic congruence can affect visuo-spatial processing and activity of the fronto-parietal attention networks, *Front. Integr. Neurosci.* 9 (2015) 45.
- [16] V. Santangelo, M. Olivetti Belardinelli, C. Spence, E. Macaluso, Interactions between voluntary and stimulus-driven spatial attention mechanisms across sensory modalities, *J. Cogn. Neurosci.* 21 (12) (2009) 2384–2397.
- [17] M.G. Veldhuizen, D. Douglas, K. Aschenbrenner, D.R. Gitelman, D.M. Small, The anterior insular cortex represents breaches of taste identity expectation, *J. Neurosci.* 31 (41) (2011) 14735–14744.
- [18] D.H. Weissman, J. Prado, Heightened activity in a key region of the ventral attention network is linked to reduced activity in a key region of the dorsal attention network during unexpected shifts of covert visual spatial attention, *NeuroImage* 61 (4) (2012) 798–804.
- [19] J.K. Wynn, A.M. Jimenez, B.J. Roach, A. Korb, J. Lee, W.P. Horan, et al., Impaired target detection in schizophrenia and the ventral attentional network: findings from a joint event-related potential-functional MRI analysis, *Neuroimage Clin.* 9 (2015) 95–102.
- [20] B. Xuan, M.A. Mackie, A. Spagna, T. Wu, Y. Tian, P.R. Hof, et al., The activation of interactive attentional networks, *NeuroImage* 129 (2016) 308–319.
- [21] M.F. Glasser, T.S. Coalson, E.C. Robinson, C.D. Hacker, J. Harwell, E. Yacoub, et al., A multi-modal parcellation of human cerebral cortex, *Nature* 536 (7615) (2016) 171–178.
- [22] A.R. Laird, J.L. Lancaster, P.T. Fox, BrainMap: the social evolution of a human brain mapping database, *Neuroinformatics* 3 (1) (2005) 65–78.
- [23] P.T. Fox, J.L. Lancaster, Opinion: Mapping context and content: the BrainMap model, *Nat. Rev. Neurosci.* 3 (4) (2002) 319–321.
- [24] P.T. Fox, A.R. Laird, S.P. Fox, P.M. Fox, A.M. Uecker, M. Crank, et al., BrainMap taxonomy of experimental design: description and evaluation, *Hum. Brain Mapp.* 25 (1) (2005) 185–198.
- [25] Q. Chen, R. Weidner, S. Vossel, P.H. Weiss, G.R. Fink, Neural mechanisms of attentional reorienting in three-dimensional space, *J. Neurosci.* 32 (39) (2012) 13352–13362.
- [26] J.T. Coull, C.D. Frith, C. Buchel, A.C. Nobre, Orienting attention in time: behavioural and neuroanatomical distinction between exogenous and endogenous shifts, *Neuropsychologia* 38 (6) (2000) 808–819.
- [27] F. Doricchi, E. Macci, M. Silvetti, E. Macaluso, Neural correlates of the spatial and expectancy components of endogenous and stimulus-driven orienting of attention in the Posner task, *Cereb. Cortex* 20 (7) (2010) 1574–1585.
- [28] J. Downar, A.P. Crawley, D.J. Mikulis, K.D. Davis, A multimodal cortical network for the detection of changes in the sensory environment, *Nat. Neurosci.* 3 (3) (2000) 277–283.
- [29] C.R. Gillebert, D. Mantini, R. Peeters, P. Dupont, R. Vandenberghe, Cytoarchitectonic mapping of attentional selection and reorienting in parietal cortex, *NeuroImage* 67 (2013) 257–272.
- [30] I. Indovina, E. Macaluso, Occipital-parietal interactions during shifts of exogenous visuospatial attention: trial-dependent changes of effective connectivity, *Magn. Reson. Imaging* 22 (10) (2004) 1477–1486.
- [31] I. Indovina, E. Macaluso, Dissociation of stimulus relevance and saliency factors during shifts of visuospatial attention, *Cereb. Cortex* 17 (7) (2007) 1701–1711.
- [32] S.J. Johnston, D.E. Linden, K.L. Shapiro, Functional imaging reveals working memory and attention interact to produce the attentional blink, *J. Cogn. Neurosci.* 24 (1) (2012) 28–38.
- [33] K. Konrad, S. Neufang, C.M. Thiel, K. Specht, C. Hanisch, J. Fan, et al., Development of attentional networks: an fMRI study with children and adults, *NeuroImage* 28 (2) (2005) 429–439.
- [34] C. Lyu, S. Hu, L. Wei, X. Zhang, T. Talhelm, Brain activation of identity switching in multiple identity tracking task, *PLoS One* 10 (12) (2015) e0145489.
- [35] E. Macaluso, C.D. Frith, J. Driver, Supramodal effects of covert spatial orienting triggered by visual or tactile events, *J. Cogn. Neurosci.* 14 (3) (2002) 389–401.
- [36] U. Mattler, T. Wustenberg, H.J. Heinze, Common modules for processing invalidly cued events in the human cortex, *Brain Res.* 1109 (1) (2006) 128–141.
- [37] A.R. Mayer, A.R. Franco, D.L. Harrington, Neuronal modulation of auditory attention by informative and uninformative spatial cues, *Hum. Brain Mapp.* 30 (5) (2009) 1652–1666.
- [38] A.R. Mayer, D. Harrington, J.C. Adair, R. Lee, The neural networks underlying endogenous auditory covert orienting and reorienting, *NeuroImage* 30 (3) (2006) 938–949.
- [39] S. Vossel, C.M. Thiel, G.R. Fink, Cue validity modulates the neural correlates of covert endogenous orienting of attention in parietal and frontal cortex, *NeuroImage* 32 (3) (2006) 1257–1264.
- [40] S. Vossel, R. Weidner, C.M. Thiel, G.R. Fink, What is “odd” in Posner’s location-cueing paradigm? Neural responses to unexpected location and feature changes compared, *J. Cogn. Neurosci.* 21 (1) (2009) 30–41.
- [41] D.C. Van Essen, M.F. Glasser, The human connectome project: progress and prospects, *Cerebrum: The Dana Forum on Brain Science* 2016, 2016 cer-10-6.
- [42] M. Larobina, L. Murino, Medical image file formats, *J. Digit. Imaging* 27 (2) (2014) 200–206.
- [43] S.B. Eickhoff, A.R. Laird, C. Grefkes, L.E. Wang, K. Zilles, P.T. Fox, Coordinate-based activation likelihood estimation meta-analysis of neuroimaging data: a random-effects approach based on empirical estimates of spatial uncertainty, *Hum. Brain Mapp.* 30 (9) (2009) 2907–2926.
- [44] S.B. Eickhoff, D. Bzdok, A.R. Laird, F. Kurth, P.T. Fox, Activation likelihood estimation meta-analysis revisited, *NeuroImage* 59 (3) (2012) 2349–2361.
- [45] P.E. Turkeltaub, S.B. Eickhoff, A.R. Laird, M. Fox, M. Wiener, P. Fox, Minimizing within-experiment and within-group effects in activation likelihood estimation meta-analyses, *Hum. Brain Mapp.* 33 (1) (2012) 1–13.
- [46] F.-C. Yeh, V.J. Wedeen, T. W-YI, Generalized Q-sampling imaging, *IEEE Trans. Med. Imaging* 29 (9) (2010) 1626–1635.
- [47] A.C. Evans, S. Marrett, P. Neelin, L. Collins, K. Worsley, W. Dai, et al., Anatomical mapping of functional activation in stereotactic coordinate space, *NeuroImage* 1 (1) (1992) 43–53.
- [48] J. Martino, P.C.D.W. Hamer, M.S. Berger, M.T. Lawton, C.M. Arnold, E.M. de Lucas, et al., Analysis of the subcomponents and cortical terminations of the perisylvian superior longitudinal fasciculus: a fiber dissection and DTI tractography study, *Brain Struct. Funct.* 218 (1) (2013) 105–121.
- [49] A. Kamali, H.I. Sair, A. Radmanesh, K.M. Hasan, Decoding the superior parietal lobule connections of the superior longitudinal fasciculus/arcuate fasciculus in the human brain, *Neuroscience* 277 (2014) 577–583.
- [50] E. Larson, A.K. Lee, The cortical dynamics underlying effective switching of auditory spatial attention, *NeuroImage* 64 (2013) 365–370.
- [51] C.M. Baker, J.D. Burks, R.G. Briggs, J.R. Sheets, A.K. Conner, C.A. Glenn, et al., A Connectomic atlas of the human cerebrum-chapter 3: the motor, premotor, and sensory cortices, *Oper. Neurosurg. (Hagerstown)* 15 (suppl.1) (2018) S75–s121.
- [52] D.H. Reser, K.J. Burman, H.H. Yu, T.A. Chaplin, K.E. Richardson, K.H. Worthy, et al., Contrasting patterns of cortical input to architectural subdivisions of the area 8 complex: a retrograde tracing study in marmoset monkeys, *Cereb. Cortex* 23 (8) (2013) 1901–1922.
- [53] M. Petrides, D.N. Pandya, Dorsolateral prefrontal cortex: comparative cytoarchitectonic analysis in the human and the macaque brain and corticocortical connection patterns, *Eur. J. Neurosci.* 11 (3) (1999) 1011–1036.
- [54] K. Nitschke, L. Kostering, L. Finkel, C. Weiller, C.P. Kaller, A meta-analysis on the neural basis of planning: activation likelihood estimation of functional brain imaging results in the tower of London task, *Hum. Brain Mapp.* 38 (1) (2017) 396–413.
- [55] M. Petrides, Lateral prefrontal cortex: architectonic and functional organization, *Philos. Trans. R. Soc. Lond. Ser. B Biol. Sci.* 360 (1456) (2005) 781–795.
- [56] E. Kirino, A. Belger, P. Goldman-Rakic, G. McCarthy, Prefrontal activation evoked by infrequent target and novel stimuli in a visual target detection task: an event-related functional magnetic resonance imaging study, *J. Neurosci.* 20 (17) (2000) 6612–6618.
- [57] R. Marois, H.C. Leung, J.C. Gore, A stimulus-driven approach to object identity and location processing in the human brain, *Neuron* 25 (3) (2000) 717–728.

- [58] C.F. Chang, T.Y. Hsu, P. Tseng, W.K. Liang, O.J. Tzeng, D.L. Hung, et al., Right temporoparietal junction and attentional reorienting, *Hum. Brain Mapp.* 34 (4) (2013) 869–877.
- [59] A.L. Berkowitz, D. Ansari, Expertise-related deactivation of the right temporoparietal junction during musical improvisation, *NeuroImage* 49 (1) (2010) 712–719.
- [60] S.C. Tyler, S. Dasgupta, S. Agosta, L. Battelli, E.D. Grossman, Functional connectivity of parietal cortex during temporal selective attention, *Cortex* 65 (2015) 195–207.
- [61] J.J. Geng, S. Vossel, Re-evaluating the role of TPJ in attentional control: contextual updating? *Neurosci. Biobehav. Rev.* 37 (10 Pt 2) (2013) 2608–2620.
- [62] M. Corbetta, G.L. Shulman, Spatial neglect and attention networks, *Annu. Rev. Neurosci.* 34 (2011) 569–599.
- [63] P. Bartolomeo, M. Thiebaut de Schotten, F. Dericchi, Left unilateral neglect as a disconnection syndrome, *Cereb. Cortex* 17 (11) (2007) 2479–2490.
- [64] B.J. He, A.Z. Snyder, J.L. Vincent, A. Epstein, G.L. Shulman, M. Corbetta, Breakdown of functional connectivity in frontoparietal networks underlies behavioral deficits in spatial neglect, *Neuron* 53 (6) (2007) 905–918.
- [65] M. Lunven, P. Bartolomeo, Attention and spatial cognition: neural and anatomical substrates of visual neglect, *Ann. Phys. Rehabil. Med.* 60 (3) (2017) 124–129.
- [66] A. Touroutoglou, M. Hollenbeck, B.C. Dickerson, L. Feldman Barrett, Dissociable large-scale networks anchored in the right anterior insula subserve affective experience and attention, *NeuroImage* 60 (4) (2012) 1947–1958.
- [67] K. Amunts, M. Lenzen, A.D. Friederici, A. Schleicher, P. Morosan, N. Palomero-Gallagher, et al., Broca's region: novel organizational principles and multiple receptor mapping, *PLoS Biol.* 8 (9) (2010).
- [68] K. Amunts, K. Zilles, Architecture and organizational principles of Broca's region, *Trends Cogn. Sci.* 16 (8) (2012) 418–426.
- [69] Y. Li, H. Yao, P. Lin, L. Zheng, C. Li, B. Zhou, et al., Frequency-dependent altered functional connections of default mode network in Alzheimer's disease, *Front. Aging Neurosci.* 9 (2017) 259.
- [70] H. Steinmetz, R.J. Seitz, Functional anatomy of language processing: neuroimaging and the problem of individual variability, *Neuropsychologia* 29 (12) (1991) 1149–1161.
- [71] S.M. Nelson, N.U. Dosenbach, A.L. Cohen, M.E. Wheeler, B.L. Schlaggar, S.E. Petersen, Role of the anterior insula in task-level control and focal attention, *Brain Struct. Funct.* 214 (5–6) (2010) 669–680.
- [72] A.D. Craig, How do you feel-now? The anterior insula and human awareness, *Nat. Rev. Neurosci.* 10 (1) (2009) 59–70.
- [73] S. Caspers, S. Geyer, A. Schleicher, H. Mohlberg, K. Amunts, K. Zilles, The human inferior parietal cortex: cytoarchitectonic parcellation and interindividual variability, *NeuroImage* 33 (2) (2006) 430–448.
- [74] S. Caspers, S.B. Eickhoff, T. Rick, A. von Kapri, T. Kuhlen, R. Huang, et al., Probabilistic fibre tract analysis of cytoarchitectonically defined human inferior parietal lobule areas reveals similarities to macaques, *NeuroImage* 58 (2) (2011) 362–380.
- [75] R.B. Mars, S. Jbabdi, J. Sallet, J.X. O'Reilly, P.L. Croxson, E. Olivier, et al., Diffusion-weighted imaging tractography-based parcellation of the human parietal cortex and comparison with human and macaque resting-state functional connectivity, *J. Neurosci.* 31 (11) (2011) 4087–4100.
- [76] P. Vrticka, J.M. Black, A.L. Reiss, The neural basis of humour processing, *Nat. Rev. Neurosci.* 14 (12) (2013) 860–868.
- [77] J.C. Culham, K.F. Valyear, Human parietal cortex in action, *Curr. Opin. Neurobiol.* 16 (2) (2006) 205–212.
- [78] M. Iacoboni, Visuo-motor integration and control in the human posterior parietal cortex: evidence from TMS and fMRI, *Neuropsychologia* 44 (13) (2006) 2691–2699.
- [79] J. Wang, Y. Yang, L. Fan, J. Xu, C. Li, Y. Liu, et al., Convergent functional architecture of the superior parietal lobule unraveled with multimodal neuroimaging approaches, *Hum. Brain Mapp.* 36 (1) (2015) 238–257.
- [80] P.H. Weiss, J.C. Marshall, K. Zilles, G.R. Fink, Are action and perception in near and far space additive or interactive factors? *NeuroImage* 18 (4) (2003) 837–846.
- [81] M. Benedek, E. Jauk, R.E. Beaty, A. Fink, K. Koschutnig, A.C. Neubauer, Brain mechanisms associated with internally directed attention and self-generated thought, *Sci. Rep.* 6 (2016) 22959.
- [82] C.L. Asplund, J.J. Todd, A.P. Snyder, R. Marois, A central role for the lateral prefrontal cortex in goal-directed and stimulus-driven attention, *Nat. Neurosci.* 13 (4) (2010) 507–512.
- [83] S.M. Szczepanski, M.A. Pinsky, M.M. Douglas, S. Kastner, Y.B. Saalmann, Functional and structural architecture of the human dorsal frontoparietal attention network, *Proc. Natl. Acad. Sci. U. S. A.* 110 (39) (2013) 15806–15811.
- [84] A. Kraft, W.H. Sommer, S. Schmidt, S.A. Brandt, Dynamic upper and lower visual field preferences within the human dorsal frontoparietal attention network, *Hum. Brain Mapp.* 32 (7) (2011) 1036–1049.
- [85] F. Scheperjans, S.B. Eickhoff, L. Homke, H. Mohlberg, K. Hermann, K. Amunts, et al., Probabilistic maps, morphometry, and variability of cytoarchitectonic areas in the human superior parietal cortex, *Cereb. Cortex* 18 (9) (2008) 2141–2157.
- [86] C.L. Colby, J.R. Duhamel, Heterogeneity of extrastriate visual areas and multiple parietal areas in the macaque monkey, *Neuropsychologia* 29 (6) (1991) 517–537.
- [87] C. Grefkes, G.R. Fink, The functional organization of the intraparietal sulcus in humans and monkeys, *J. Anat.* 207 (1) (2005) 3–17.
- [88] D. Bzdok, A. Heeger, R. Langner, A.R. Laird, P.T. Fox, N. Palomero-Gallagher, et al., Subspecialization in the human posterior medial cortex, *NeuroImage* 106 (2015) 55–71.
- [89] A.E. Cavanna, M.R. Trimble, The precuneus: a review of its functional anatomy and behavioural correlates, *Brain* 129 (3) (2006) 564–583.
- [90] P.G. Allan, R.G. Briggs, A.K. Conner, C.M. O'Neal, P.A. Bonney, B.D. Maxwell, et al., Parcellation-based tractographic modeling of the dorsal attention network, *Brain Behav.* 9 (10) (2019) 1–14.
- [91] S. Rossi, S. Huang, S.C. Furtak, J.W. Belliveau, J. Ahveninen, Functional connectivity of dorsal and ventral frontoparietal seed regions during auditory orienting, *Brain Res.* 1583 (2014) 159–168.
- [92] D. Sridharan, D.J. Levitin, C.H. Chafe, J. Berger, V. Menon, Neural dynamics of event segmentation in music: converging evidence for dissociable ventral and dorsal networks, *Neuron* 55 (3) (2007) 521–532.